Chain conformations dictate multiscale charge transport phenomena in disordered semiconducting polymers

Rodrigo Noriega[a,1], Alberto Salleo[b], and Andrew J. Spakowitz[c,2]

Departments of [a]Applied Physics, [b]Materials Science and Engineering, and [c]Chemical Engineering, Stanford University, Stanford, CA 94305

Edited by Mark A. Ratner, Northwestern University, Evanston, IL, and approved August 28, 2013 (received for review April 23, 2013)

Existing models for the electronic properties of conjugated polymers do not capture the spatial arrangement of the disordered macromolecular chains over which charge transport occurs. Here, we present an analytical and computational description in which the morphology of individual polymer chains is dictated by well-known statistical models and the electronic coupling between units is determined using Marcus theory. The multiscale transport of charges in these materials (high mobility at short length scales, low mobility at long length scales) is naturally described with our framework. Additionally, the dependence of mobility with electric field and temperature is explained in terms of conformational variability and spatial correlation. Our model offers a predictive approach to connecting processing conditions with transport behavior.

organic electronics | charge mobility | computational model

The performance of organic semiconductors has improved substantially in recent years through careful molecular engineering and processing (1, 2), and solution-processed systems are now competitive with amorphous silicon. A path to constant improvement is best guided by rational materials design, which requires that the relationship between processing, structure, and ensuing properties be well understood. In complex macromolecular systems, such as conjugated polymers, there is no generally accepted model for charge transport that explicitly takes into account the macromolecular nature of the material. Such difficulty is partially due to their complicated microstructural behavior and strongly disordered intramolecular conformation and intermolecular packing.

Several properties of flexible macromolecules are understood in terms of the statistics of their chain conformations. For example, the viscoelasticity of polymers in solution has been shown to depend on chain entanglements (3–5), and liquid-crystalline microstructures result from nematic ordering of individual chains (6). We present a model of electrical charge transport in conjugated polymers that places this important property on the same theoretical footing as many other macromolecular properties. To achieve this goal, it is necessary to build the model by starting from the polymer and its disordered conformations.

The disordered nature of semiconducting polymers is rationalized to be the cause of many observations in these systems, most notably thermally activated charge transport attributed to disorder-induced traps (7, 8). On-site energetic disorder and positional disorder are invoked in phenomenological models to explain the dispersive nature of charge transport and the electric-field dependence of charge mobility (i.e., the Poole–Frenkel effect), often including intersite correlations (8, 9).

Gaussian disorder models (GDMs) are based on describing a 3D material as a grid of sites. The on-site energy is selected from a Gaussian probability distribution to reflect the energetic disorder in the material. Structural disorder is introduced by varying the localization radius of each site's wavefunction, affecting intersite transfer. This model can be modified to include spatial correlations in on-site energies, which provides an explanation for the electric-field dependence of charge mobility over a larger range in electric field strength (10, 11). Great progress in device modeling and materials understanding has resulted from applying Gaussian disorder models, partly due to their ability to be incorporated into advanced computational simulations. Initially, Gaussian disorder models were developed to study charge transport in molecularly doped systems or amorphous small molecules, where the electronic coupling between individual sites is small and isotropic (12–14). The importance of disorder for charge transport in conjugated polymers resulted in the application of the same GDM framework (15). However, for conjugated polymer materials, the applicability of models developed for molecularly doped systems is not clear, and a physical understanding of the underlying molecular mechanism behind disorder is still lacking.

Recent experimental measurements reveal the fundamentally multiscale nature of charge transport in semiconducting polymers—fast motion at short length scales and slow motion at large length scales—and show its deep relationship to the hierarchical connectivity of their macromolecular structure (16–18). Indeed, a charge can move quickly along a single chain but may have to wait a long time before being able to hop from chain to chain.

This observation highlights one of the shortcomings of the GDM-based framework currently used to describe charge transport in conjugated polymers: it cannot account for the fine-grained mechanism of charge transfer through a disordered polymer film. These models have been successful at describing long-range transport due to the coarsening of the microstructure at such length scales. Although a time-dependent mobility might be extracted in the process of energy relaxation in the density of states in a GDM, this process is fundamentally different from providing a multiscale description of the mobility. In a conjugated polymer, even after a charge has traversed a large number of chains, its motion will still be described as fast at short distances

Significance

Semiconducting polymers have promising applications in transistors, light-emitting diodes, and solar cells. These materials have microstructures that exhibit heterogeneity over multiple length scales, which obscures the relationship between properties, processing conditions, and device performance. Our work provides a theoretical framework to address the role of polymer conformations in electronic transport through disordered semiconducting polymers. We present a simple model that reconciles observations at the local scale with device-scale measurements of charge mobility (charges move quickly at short distances and slowly at long distances). The main features are the use of well-known models to describe the conformations of individual polymer chains and the inclusion of the kinetics of electronic transport between sites on a single polymer and between adjacent chains.

Author contributions: A.J.S. designed research; R.N. performed research; R.N., A.S., and A.J.S. analyzed data; and R.N., A.S., and A.J.S. wrote the paper.

The authors declare no conflict of interest.

This article is a PNAS Direct Submission.

[1]Present address: Department of Chemistry, University of California, Berkeley, CA 94720.

[2]To whom correspondence should be addressed. E-mail: ajspakow@stanford.edu.

This article contains supporting information online at www.pnas.org/lookup/suppl/doi:10.1073/pnas.1307158110/-/DCSupplemental.

and slow at long distances. Thus, we arrive at the root of the problem: differences in electronic coupling between sites on the same chain and those on different polymer chains are not included in present charge transport models. In this manuscript, we present a charge transport model that provides a microscale interpretation of the impact of polymer conformations on intrachain and interchain transport processes.

By developing a model that includes the inherent structural features of individual chains and the statistical behavior of an ensemble of such chains, it is possible to provide a more fundamental description of charge transport in disordered semiconducting polymers. Here, we explore the role of individual chain conformation as the key feature dominating the way charges move in solid films of disordered semiconducting polymers. Our model reconciles the observed multiscale transport behavior with temperature- and field-dependent mobility measurements. This framework provides physical insights capable of guiding materials design and offers a predictive approach to connecting processing conditions with transport behavior. Additionally, the treatment described here can be used as a building block to study intergrain transport in semicrystalline materials. The simple theoretical treatment described here is an improvement upon current charge transport models, and recent molecular dynamics (MD) and density functional theory (DFT) calculations (19) confirm several inherent features of our theory. These MD and DFT calculations show that the electronic structure of amorphous polymers can be determined by the disordered conformations of individual chains, and that the interaction between electronic states localized in the same chain or in adjacent chains is different.

Model

Our model first addresses the conformations of polymer chains in a disordered amorphous solid. At small length scales, a polymer chain in such materials exhibits rod-like correlation in their orientation, reflecting the molecular elasticity of the segments of the chain. At much larger length scales, the additive effect of small local deformations results in a conformation resembling a random walk. This semiflexible behavior is common to many polymer systems and is essential in capturing the multiscale transport behavior in conjugated polymer materials.

Semiflexible polymer chains can be described by the worm-like chain model (20–26). The orientation of the chain at each point is defined by the tangent vector $\vec{u}$, which has unit magnitude to enforce chain inextensibility arising from stiff covalent segmental bonds. The degree to which a given chain resists deformation is reflected in its persistence length l_p, which is the distance over which the tangent vectors $\vec{u}$ are correlated. The Hamiltonian for a worm-like chain is given by the following:

$$\frac{\mathcal{H}}{k_BT}=\frac{l_p}{2}\int_0^L\left(\frac{\partial\vec{u}}{\partial s}\right)^2 \mathrm{d}s, \qquad [1]$$

where k_BT is the thermal energy, L is the contour length of the polymer chain, and s is the path length coordinate along the chain ($s=0$ at one end, and $s=L$ at the opposite end).

For simulations, we discretize the chain into segments of length l_0. Upon discretization, the bending modulus $\epsilon=l_p/l_0$ governs the resistance to bending between adjacent discrete subunits. To reproduce the properties of a solid amorphous film, a random sample of all possible conformations is selected, where the bending between segments follows Boltzmann statistics. Because the amorphous material is assumed to be prepared from a concentrated polymer solution, we assume the chain configurations obey ideal chain statistics that are unaffected by segmental interactions (27–29). The polymer chains are assumed to be fixed in the amorphous material, which exists in either a semicrystalline solid state or a quenched glassy state. Our model focuses on the disordered amorphous state due to the experimental systems that are the focus in this study, but future work will address semicrystalline materials (see *SI Text* for details regarding the selection of polymer conformations).

Fig. 1 provides a schematic representation of each level in our hierarchical model for charge transport. Fig. 1*A* shows two randomly generated chains (one in blue, the other in red) to describe various aspects of the proposed model. The semiflexible behavior of polymer chains is evidenced, and the distances corresponding to the persistence length l_p and segment length l_0 are shown. An electric field $\vec{F}$ breaks the symmetry of the system and defines a preferential direction for charge motion. Each site can transfer charge to its two neighbors on the same chain with rates k_i^+ (for transfer from site i to $i+1$) and k_i^- (for transfer from site i to $i-1$), and to a different chain with rate k_{hop}. The energetic landscape a charge experiences when moving along a semiflexible chain in the presence of an electric field is affected by the polymer conformation. For simplicity and without loss of generality, the direction of the electric field $\vec{F}=F\hat{z}$ is taken along the z axis. Fig. 1*B* shows a polymer chain with monomer coloring to indicate the z position of each monomer, where red is the maximum z position in the chain and blue is the minimum z position. The corresponding electrostatic potential energy of a charge at each monomer position is shown in Fig. 1*C*. Even though the overall behavior is to lower the charge's electrostatic energy by moving along the chain, short- and medium-range conformation fluctuations can act as barriers for charge transport.

The electronic properties are determined based on the spatial arrangement of the polymer segments. The transfer rates between the discretized sites of the chain are calculated using Marcus theory (30, 31). Without including inherent variations in site energy, a charge q experiences an energy difference ΔG_{ij} between sites i and j resulting from their positions along the electric field. This energy difference is given by $\Delta G_{i,j}=-Fq(z_j-z_i)$, where z_i is the z position of the ith polymer segment. Using semiclassical Marcus theory (30, 31), the transfer rate for hopping from site i to site $i+1$ on the same chain is as follows:

$$k_{i,i+1}=k_i^+=\frac{2\pi}{\hbar}\frac{J_0^2}{\sqrt{4\pi\lambda_0k_BT}}\exp\left[-\frac{\left(\lambda_0+\Delta G_{i,i+1}\right)^2}{4k_BT\lambda_0}\right], \qquad [2]$$

where J_0 is the electronic coupling between neighboring sites in the chain, λ_0 is the reorganization energy, and $\hbar$ is the reduced Planck's constant. Similarly, the transfer rate from site i to site $i-1$ on the same chain is as follows:

$$k_{i,i-1}=k_i^-=\frac{2\pi}{\hbar}\frac{J_0^2}{\sqrt{4\pi\lambda_0k_BT}}\exp\left[-\frac{\left(\lambda_0+\Delta G_{i,i-1}\right)^2}{4k_BT\lambda_0}\right]. \qquad [3]$$

Each site can also couple to another site on a different chain, with a rate k_{hop} determined by the interchain electronic coupling J_{hop} and a reorganization energy λ_{hop}. We assume a constant negative energy difference $\Delta G_{hop}=-Fq\gamma l_0$ for interchain transfer, where γ is the ratio between the interchain hop distance and the segment length l_0. The validity of Marcus theory is not central to our treatment of charge transfer events; any rate equation that satisfies detailed balance and is parametrizable can be applied (e.g., Miller–Abrahams).

We now use this framework to study charge transport applying two different approaches. First, we focus on the limiting case where charges move large distances. This limit is relevant because in typical experiments charges move distances longer than any individual chain over timescales much longer than the hopping time between chains. Later, we pay closer attention to the processes of charge transport at smaller length scales and faster timescales, following the transfer of charge between individual conjugated segments.

At any point in the simulation, only one chain is under consideration, and the escape from the chain is described with an effective rate that is independent from the location of other chains. This simplification is valid in the low charge density regime, and given the strong anisotropy in electronic coupling

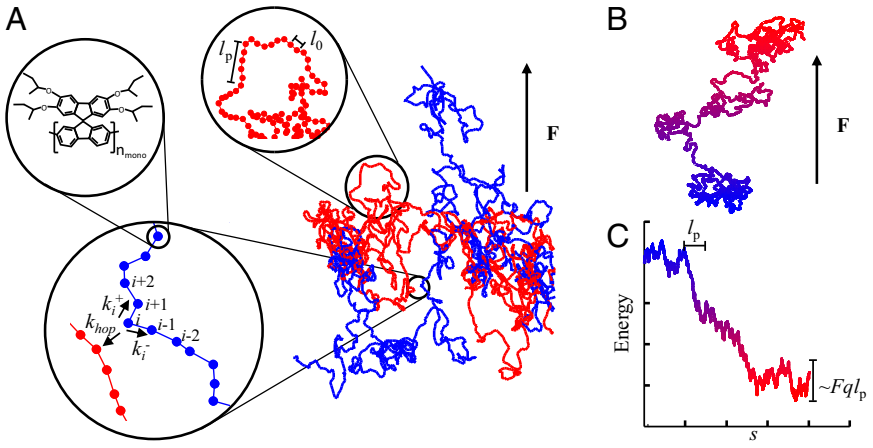

Fig. 1. Schematic representation of our model for charge transport in conjugated polymers. (*A*) Hierarchical representation demonstrating the multiscale features built into our model. (*B* and *C*) The effect of chain conformation on the energetic landscape experienced by a charge within the conjugated polymer.

observed in this study, intrachain transfer is much faster than interchain hopping, and the electric field imparts a strong directionality to interchain hopping. Thus, the probability of returning to a previous chain is ignored, and assumed that each interchain hop can be treated as arriving at a new configuration.

When a charge is placed on a polymer chain, a set of rate equations describe the time evolution of the probability of occupying each site along the chain as a function of time, given by the following:

$$\frac{dp_i}{dt} = -p_i\left(k_{hop} + k_i^+ + k_i^-\right) + p_{i-1}k_{i-1}^+ + p_{i+1}k_{i+1}^-, \qquad [4]$$

where the first term on the right-hand side describes hopping from site i to either a new chain or to neighboring sites $i \pm 1$ on the same chain, and the last two terms on the right-hand side represent hopping to site i from the same neighboring sites $i \pm 1$. The hopping rates are calculated for each chain conformation as a function of temperature and applied electric field.

The long-time limit allows a simplification of the governing equation describing charge motion (Eq. **4**). The Laplace transform of this coupled set of differential equations is defined as follows:

$$\tilde{p}_i(\nu) = \int_0^\infty p_i(t)\exp(-t\nu)dt. \qquad [5]$$

The transform evaluated at $\nu = 0$ is equivalent to integrating the probability of occupying each site over all time. For each new polymer chain, the charge is initially placed in a randomly selected site along the chain. Solving the coupled set of algebraic equations for $\tilde{p}_i(\nu = 0)$, and normalizing the probabilities by the rate at which they decay (interchain hopping rate k_{hop}), we calculate the expected value of the position at which the charge will exit the chain at long times. It is thus possible to calculate the displacement of the charge in the polymer chain between hopping events, or its drift length. Repeating this process for a large number of chains, the ensemble average of single-occupancy drift lengths $\langle z \rangle$ is calculated. Expressing the average charge speed as the single-occupancy drift length divided by the average interchain hopping time $(1/k_{hop})$, we obtain $\langle v \rangle = k_{hop}\langle z \rangle$. This average speed can then be used to calculate the charge mobility if we divide by the electric field F, $\mu = k_{hop}\langle z \rangle / F$ (see *SI Text* for details).

Besides focusing on the long-time behavior of charges, our framework is ideally suited to study charge transport at much smaller length scales and faster timescales. This behavior is observed by tracking the position of individual charges as they hop between conjugated subunits using a dynamic Monte Carlo simulation, implementing the Gillespie algorithm (32, 33) for the hopping events. At every point in time the charge resides on one site of a chain (i), and it can undergo three distinct charge transfer reactions. The charge can hop to the neighboring sites $(i \pm 1)$ on the same chain with rates $k_i^\pm$ or to a different chain with rate k_{hop}. When the charge hops to a new chain, it arrives at a randomly selected site along this new randomly determined chain configuration. The result of each reaction is chosen at random, where each possible outcome is weighted by its transfer rate (i.e., reactions with faster transfer rates are more likely). The reaction time is selected randomly from an exponential distribution with decay rate $k_{tot} = k_{hop} + k_i^+ + k_i^-$. Allowing each charge to move through many individual chains and averaging the trajectories of many charges yields the ensemble-average charge transport rate. The long-time value of the charge transport rate tends to the value determined using the Laplace-transform methodology. In addition to the long-time limit, the Monte Carlo methodology provides a history of the charge transport at different time and length scales (see *SI Text* for details).

Before detailing the results of our approach, it is useful to describe the characteristics that set it apart from the other available models. First and most important, it incorporates a better approximation to the physical nature of the semiconducting material, with a simple model to describe the polymer chains. The model accounts for the fact that each site where charges reside is part of a larger macromolecular chain, with a strongly anisotropic connectivity to other sites determined by its position within the chain. Moreover, the conformation of individual chains is obtained from fundamental materials parameters and is the result of small bends of the polymer backbone. In this regard, our model is easily extended to include a more detailed treatment of the processing conditions and the molecular interactions that govern the solid-state microstructure.

Bridging the gap between electronic and microstructural modeling provides a more realistic inclusion of the different processes that result in macroscopic charge transport in disordered conjugated polymers. However, there are some aspects that this version of the model neglects. The effect of bending and twisting the polymer backbone on the electronic coupling is not included. A distribution of conjugation lengths (or segment lengths) is to be expected in any real material, which could result as well in variations in the on-site energies. These effects are neglected with the objective of keeping the model as simple as possible and are justifiable on the basis of modeling strongly disordered materials in which chain conformation is the limiting factor to charge transport.

Thermally Activated Transport and Poole–Frenkel Effect

With the long-time limit approach described above, we study two well-known phenomena in organic semiconductors: thermally activated transport and the Poole–Frenkel effect (electric-field–dependent charge mobility). We explain the molecular mechanism

that gives rise to both of these observations and reveal the key role of disordered chain conformations. A set of time-of-flight measurements of the mobility of poly(spiro-bifluorene) reported by Laquai et al. (34) is shown in Fig. 2*A*. It is important to note the evident thermal activation of transport and a dependence of mobility with electric field. The original data were modeled with a Gaussian disorder model (Eq. **6**), using an intersite distance of 0.6 nm, a width of the distribution of on-site energies of $\sigma = 86$ meV, a mobility prefactor $\mu_0 = 2.9 \times 10^{-4}$ cm^2/Vs, and an exponential field dependence $C_0 = 3.5 \times 10^{-4}(\mathrm{cm/V})^{\frac{1}{2}}$.

$$\mu = \mu_0 \exp\left[\left(\frac{2\sigma}{3k_BT}\right)^2\right] \exp\left[C_0\left(\frac{\sigma}{k_BT}\right)^2\sqrt{F}\right]. \qquad [6]$$

With our model, the basic physics of the experiment can be described using a semiflexible chain of $N = 201$ beads, each representing a monomer with an interbead spacing $l_0 = 0.9 \pm 0.2$ nm and bending modulus $\epsilon = 1.7 \pm 1.0$ (persistence length $l_p = 1.6$ nm). The intrachain transfer rates are determined by $J_0 = 46 \pm 23$ meV and $\lambda_0 = 644 \pm 58$ meV, and the interchain transfer parameters are $J_{hop} = 0.34 \pm 0.05$ meV, $\lambda_{hop} = 799 \pm 30$ meV, and $\gamma = 5.6 \pm 0.6$. These values are obtained with a simulated annealing routine to explore a large parameter space through random perturbations to the fitting parameters (see *SI Text* for details).

The values obtained with this approach are reasonable for a flexible polymer with weakly coupled electronic units, such as poly(spirobifluorene). The persistence length of more rigid polyalkyl fluorenes is on the order of 7 nm (35), but the spiro linkage disrupts molecular packing and reduces the persistence length to only a few monomer units. The reorganization energies of a few hundred millielectronvolts and electronic couplings of a few millielectronvolts agree well with recent calculations in a variety of systems (36–39). A recent study of phenanthrene indenofluorene copolymers suggests that reorganization energies are lower than those calculated by DFT, so disorder and hole localization effects are predominant (40). Introducing a small amount of energetic disorder (35 meV) to our simulations resulted in lower reorganization energies but no change in the remaining fitting parameters.

Several additional metrics are commonly used to analyze measurements of charge mobility versus external field and temperature. One of such metrics is the field dependence of the mobility at a constant temperature, captured by $\beta = d(\log \mu)/d(\sqrt{F})$. Fig. 2*B* provides experimental and theoretical values for β. It can be seen that our model accurately predicts the behavior of β versus $1/T^2$. Fig. 2*B* is a reasonable way to display the data because the Poole–Frenkel effect predicted by Gaussian disorder models typically results in linear plots when the data are represented in this manner (Eq. **6**) (34).

Spatial correlations in the site energies for Gaussian disorder models have been used to describe the dependence of charge mobility on electric field. One explanation for the origin of such correlations relies on the large polarizability of organic molecules to create a disordered dipole arrangement that results in correlated on-site energies (10, 11). Conversely, by averaging over a large ensemble of randomly generated chains, we can use our charge transport model for disordered conjugated polymers to offer an explanation for these correlations within a disordered energetic landscape.

A randomly selected pair of nearest neighbors have any orientation with respect to the electric field with equal probability. However, once a charge is placed on a given site on a chain it is able to travel a certain distance Δz along the field direction before encountering a bend in the chain that acts as a transport barrier. Upon arriving at the bend, the charge must either wait to overcome the barrier or hop to a neighboring chain. This distance Δz follows an exponential distribution with a decay length dictated by the distance over which the orientation of individual segments is correlated, i.e., the persistence length l_p. In other words, once the charge is placed on a segment of a chain with a finite bending modulus, the orientation of the neighboring segments are correlated due to the intrinsic molecular elasticity of the chain, leading to energetic correlations for charge transport.

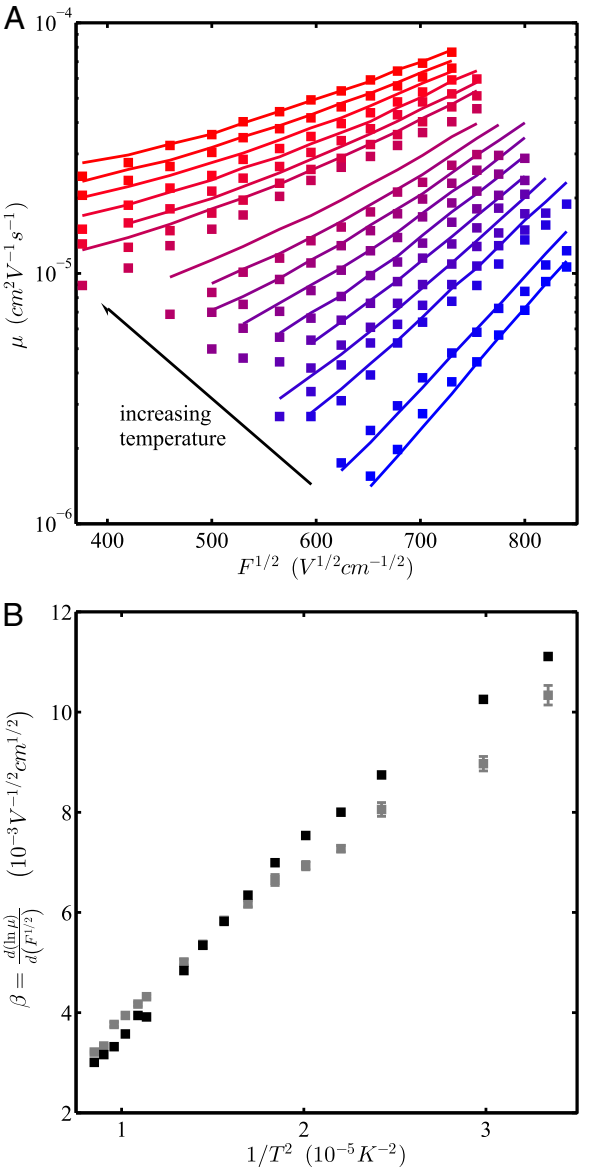

Fig. 2. Modeling of time-of-flight mobility of spirobifluorene. (*A*) The data as reported by Laquai et al. (34) is shown by squares, color coded by temperature (from 173 K to 343 K). The solid lines are results obtained with our model. (*B*) The slope of logarithmic plots of mobility vs. the square root of the electric field is a useful metric to compare models and experimental data. The error bars are obtained as the SE of fitting a line to a logarithmic plot of the raw data.

Multiscale Behavior of Charge Transport

Using dynamic Monte Carlo simulations, we study the behavior of charges as they move through a set of disordered polymer chains. With this analysis, two very different regimes are observed (Fig. 3). At short times, charges move short distances with a large mobility along the polymer backbone, and at longer times, charge move larger distances with a much lower mobility corresponding to multiple interchain hops. The transition between these two regimes happens after the charges have moved a distance on the order of the persistence length along the chain backbone and do so in a time consistent with the interchain hopping rate.

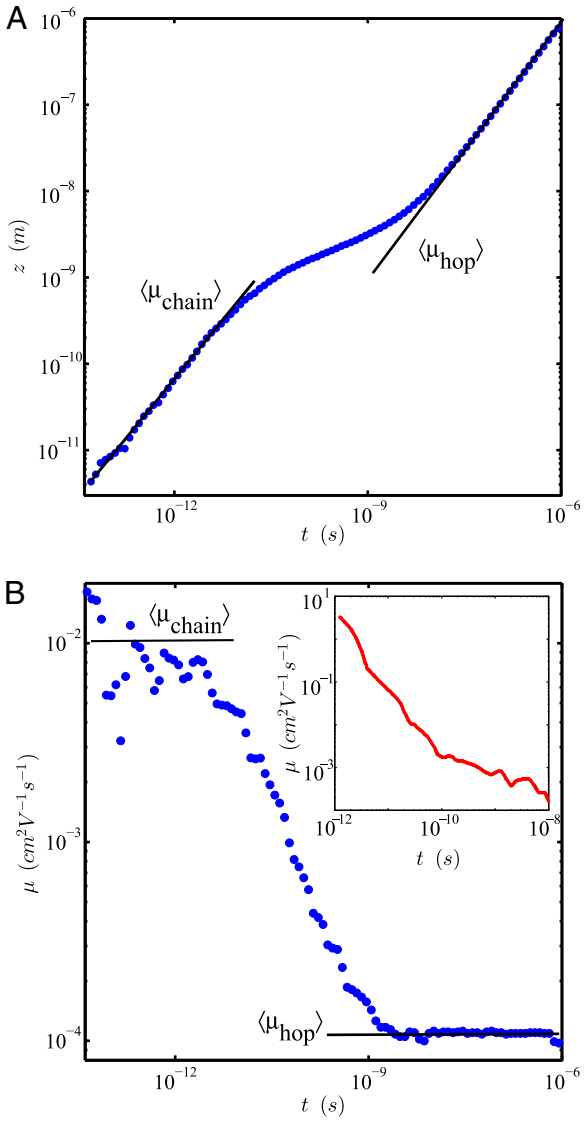

Fig. 3. Monte Carlo simulations of the multiscale behavior of charges in conjugated polymers. Ensemble average of the position (*A*) and mobility (*B*) as a function of time after injection or excitation of charges as obtained with computer simulations for poly(spirobifluorene). These simulations assumed a film thickness of 100 nm, an applied voltage of 8 V, and a temperature of 300 K. The *Inset* shows experimental results of mobility as a function of time after charge injection obtained by Devizis et al. (18) for a ladder-type polymer (MeLPPP).

This multiscale behavior of charges has been previously observed experimentally by several groups using pulse-radiolisis time-resolved microwave conductivity or time-resolved electric field-induced second harmonic generation, but its explanation has remained at a qualitative level (16, 18, 34, 41). Fast transport along a single conjugated backbone has been cited as the reason for a large mobility at short times and for short distances in a variety of materials, but the addition of ad hoc time dependence in the GDM has been used to model the data. Our framework provides a detailed quantitative explanation of this behavior, relating it to fundamental materials properties. It is important to compare our simulations for spirobifluorene with experimental results obtained by Devizis et al. (18) for a ladder-type polymer, methyl-substituted ladder-type poly(para-phenylene) (MeLPPP) (Fig. 3, *Inset*). The resemblance between the two behaviors is remarkable, with the differences in mobility and timescales arising from differences in the electronic and mechanical properties of the two materials. MeLPPP is much more rigid than poly (spirobifluorene)—with a persistence length of 25 nm (35)—which increases the on-chain electronic coupling.

It is possible to arrive at an analytical expression for the on-chain mobility by using the fact that any randomly selected pair of neighbors has an equal probability of pointing in any direction with respect to the electric field. Thus, the component of the velocity of a charge along the field direction can be written as the rate for transfer (k_{intra}) times the displacement ($l_0 \cos\theta$) and averaged over all possible values. This expression (*SI Text*) depends only on the parameters describing on-chain transport (J_0, λ_0, and l_0) as well as on the electric field and temperature. The value obtained with this analytical approach agrees very well with the results from simulations (Fig. 3*B*) and provides additional validation for the interpretation of the mechanisms at play in the hierarchical charge transport process in conjugated polymers.

Because the hopping rates and the electrostatic barriers for charge transport will be dependent on the temperature and electric field, charges will behave differently as these parameters change. Systematic studies of charge transport across a variety of timescales as a function of electric field and temperature will allow the precise determination of fundamental materials parameters at play in charge transport, and guide materials design.

It is important to note that the electronic properties of semiconducting polymers are not completely described by device-scale measurements (e.g., transistor transfer curves), but the multiscale nature of charge transport processes in these systems requires complementary techniques that explore local charge transfer mechanisms [e.g., time-resolved electric-field–induced second harmonic generation (16–18), pulse radiolysis time-resolved microwave conductivity (41), THz pump-probe (42)]. Here, we describe a simple model that is capable of connecting these disparate length and time scales to experimentally and chemically accessible materials properties.

Being able to relate changes in the electronic properties or processing conditions of a material to the observable charge transport behavior is of great importance in the development and improvement of semiconducting polymers. If the goal is to improve local charge transport, the most important parameter to tune is the intrachain electronic coupling. This approach would be useful to avoid charge recombination at an interface in organic photovoltaics, where one wants charges to move a few nanometers quickly. However, if the goal is to improve the transport of charge at the device scale, then the most effective approach lies in processing of the material, aligning the chains to use the more efficient intrachain transport to increase the drift length of charges in each polymer chain. Such drastic improvements in conductivity of conjugated polymers with mechanical stretching have been experimentally observed previously (43). Tuning the interchain electronic coupling also results in significant improvements in the long-range charge mobility, with little effects on the ultrafast intrachain charge transport. The dependence of charge transport on several materials parameters is described in more detail in *SI Text* (Fig. S1).

Conclusions

With the structural considerations included in this model, a more complete view of charge transport in disordered semiconducting polymers becomes available. One of the prominent features of the model discussed in this manuscript is the common structural origin of experimental observations that have usually been explained with two distinct phenomenological models. These two experimental observations are as follows: (*i*) the temperature and electric field dependence of mobility in macroscopic measurements, and (*ii*) the remarkably high mobility of charges at short length scales, and a transition to lower mobility for larger displacements. The inherent hierarchical nature in the connectivity of individual polymer segments, and variations in local chain conformation of disordered polymer semiconductors can explain the behavior of charges in these systems at both limiting cases.

Although it is designed to model disordered polymers, this framework can be extended to more ordered systems by modifying the microstructural description of the chains. For example, the semidisordered region between aggregates in high-mobility

semicrystalline polymers is composed of distorted (but not entirely amorphous) chains that provide connectivity between the ordered regions. Additional modifications to this model may result from realizing that, if chain conformation is so distorted that large bends are possible, it should affect the electronic coupling between units along the conjugated backbone. Moreover, the model presented here can be extended to describe different systems where anisotropic and multicomponent transport is observed, with significant modifications. One of such systems is networks of rigid inorganic nanowires or of more flexible carbon nanotubes (44–48). These networks are sparse, which results in a key difference from the model we propose. In polymer films, it is reasonable to assume that charges can hop to a new chain at any point along the chain (i.e., every site has a nearby neighbor that belongs to a different chain). In sparse nanotube networks, not every point along the nanotube has the potential to transfer charge to another nanotube. Another related system is the study of diffusive transport through polymeric materials, which can involve transient binding to the polymer chains and consequently anomalous transport behavior. For example, such effects are implicated in protein transport through crowded DNA networks to facilitate the binding to specific DNA sites (48–50). The trapping of charges in our model is a result of the external field and would not arise for passive diffusive transport. These related physical systems share the common feature of having complex transport trajectories that are dictated by chain conformation and layout, and our model offers insight into how these effects can be addressed in a simple theoretical framework.

The inclusion of the macromolecular nature of conjugated polymers in the description of charge transport is a definitive step to increase the understanding of the fundamental materials properties at play, and the multiscale processes that must take place to sustain efficient macroscopic charge transport. Furthermore, the model described here provides physical insights capable of guiding materials design and offers a predictive approach to connecting processing conditions with transport behavior.

ACKNOWLEDGMENTS. We thank H. Bässler for his comments in the preparation of this manuscript. This work is partially supported by the Center for Advanced Molecular Photovoltaics Award KUS-C1-015-21 made by King Abdullah University of Science and Technology (to R.N. and A.S.), and the National Science Foundation (A.S.). A.J.S. acknowledges funding support from the School of Engineering at Stanford University.

1. Yan H, et al. (2009) A high-mobility electron-transporting polymer for printed transistors. *Nature* 457(7230):679–686.
2. Bronstein H, et al. (2012) Indacenodithiophene-co-benzothiadiazole copolymers for high performance solar cells or transistors via alkyl chain optimization. *Macromolecules* 44(17):6649–6652.
3. Piechocka IK, Bacabac RG, Potters M, Mackintosh FC, Koenderink GH (2010) Structural hierarchy governs fibrin gel mechanics. *Biophys J* 98(10):2281–2289.
4. Spakowitz AJ, Wang Z-G (2003) Semiflexible polymer solutions. I. Phase behavior and single-chain statistics. *J Chem Phys* 119(24):13113–13128.
5. Pasquali M, Shankar V, Morse DC (2001) Viscoelasticity of dilute solutions of semiflexible polymers. *Phys Rev E* 64(2):020802.
6. Chen ZY (1993) Nematic ordering in semiflexible polymer chains. *Macromolecules* 26(13):3419–3423.
7. Baranovskii S (2006) *Charge Transport in Disordered Solids with Applications in Electronics* (John Wiley & Sons, Ltd, Chichester, United Kingdom).
8. Bässler H (1993) Charge transport in disordered organic photoconductors—a Monte Carlo simulation study. *Physica Statuts Solidi B* 175(1):15–56.
9. Tessler N, Preezant Y, Rappaport N, Roichman Y (2009) Charge transport in disordered organic materials and its relevance to thin-film devices: A tutorial review. *Adv Mater* 21(27):2741–2761.
10. Parris PE, Dunlap DH, Kenkre VM (2000) Energetic disorder, spatial correlations, and the high-field mobility of injected charge carriers in organic solids. *Phys Status Solidi B Basic Res* 218(1):47–53.
11. Gartstein YN, Conwell EM (1995) High-field hopping mobility in molecular systems with spatially correlated energetic disorder. *Chem Phys Lett* 245(4-5):351–358.
12. Reimer B, Bässler H (1979) Fast hole transport in polyvinylcarbazole. *Phys Status Solidi A Appl Res* 51(2):445–451.
13. Bässler H (1981) Localized states and electronic transport in single component organic solids with diagonal disorder. *Phys Status Solidi B Basic Res* 107(1):9–54.
14. Borsenberger PM, Pautmeier L, Bässler H (1991) Disordered molecular solids. *J Chem Phys* 94(8):5447–5454.
15. Binh NT, Minh LQ, Bässler H (1993) Photoconduction in poly(3-alkylthiophene). II. Charge transport. *Synth Met* 58(1):39–50.
16. Devizis A, Serbenta A, Meerholz K, Hertel D, Gulbinas V (2009) Ultrafast dynamics of carrier mobility in a conjugated polymer probed at molecular and microscopic length scales. *Phys Rev Lett* 103(2):027404.
17. Devizis A, Meerholz K, Hertel D, Gulbinas V (2010) Ultrafast charge carrier mobility dynamics in poly(spirobifluorene-co-benzothiadiazole): Influence of temperature on initial transport. *Phys Rev B* 82(15):155204.
18. Devizis A, Meerholz K, Hertel D, Gulbinas V (2010) Hierarchical charge carrier motion in conjugated polymers. *Chem Phys Lett* 498(4-6):302–306.
19. Qin T, Troisi A (2013) Relation between structure and electronic properties of amorphous MEH-PPV polymers. *J Am Chem Soc* 135(30):11247–11256.
20. Yamakawa H (1997) *Helical Wormlike Chains in Polymer Solutions* (Springer, Berlin).
21. Van Der Maarel JRC (2008) *Introduction to Biopolymer Physics* (World Scientific, Singapore).
22. Spakowitz AJ, Wang Z-G (2004) Exact results for a semiflexible polymer chain in an aligning field. *Macromolecules* 37(15):5814–5823.
23. Spakowitz AJ, Wang Z-G (2005) End-to-end distance vector distribution with fixed end orientations for the wormlike chain model. *Phys Rev E Stat Nonlin Soft Matter Phys* 72(4 Pt 1):041802.
24. Spakowitz AJ (2006) Wormlike chain statistics with twist and fixed ends. *Europhys Lett* 73(5):684.
25. Mehraeen S, Sudhanshu B, Koslover EF, Spakowitz AJ (2008) End-to-end distribution for a wormlike chain in arbitrary dimensions. *Phys Rev E Stat Nonlin Soft Matter Phys* 77(6 Pt 1):061803.
26. McCulloch B, et al. (2013) Polymer chain shape of poly(3-alkylthiophenes) in solution using small-angle neutron scattering. *Macromolecules* 46(5):1899–1907.
27. Flory P (1953) *Principles of Polymer Chemistry* (Cornell Univ Press, Ithaca, NY).
28. de Gennes P-G (1979) *Scaling Concepts in Polymer Physics* (Cornell Univ Press, Ithaca, NY).
29. Rubinstein M, Colby RH (2003) *Polymer Physics* (Oxford Univ Press, Oxford).
30. Marcus RA, Sutin N (1975) Electron-transfer reactions with unusual activation parameters - treatment of reactions accompanied by large entropy decreases. *Inorg Chem* 14(1):213–216.
31. Marcus RA, Sutin N (1985) Electron transfers in chemistry and biology. *Biochim Biophys Acta* 811(3):265–322.
32. Gillespie DT (1977) Exact stochastic simulation of coupled chemical reactions. *J Phys Chem* 81(25):2340–2361.
33. Gillespie DT (1976) A general method for numerically simulating the stochastic time evolution of coupled chemical reactions. *J Comput Phys* 22(4):403–434.
34. Laquai F, Wegner G, Bässler H (2007) What determines the mobility of charge carriers in conjugated polymers? *Philos Trans A Math Phys Eng Sci* 365(1855):1473–1487.
35. Grimsdale AC, Mullen K (2007) Oligomers and polymers based on bridged phenylenes as electronic materials. *Macromol Rapid Commun* 28(17):1676–1702.
36. Hutchison GR, Ratner MA, Marks TJ (2005) Hopping transport in conductive heterocyclic oligomers: Reorganization energies and substituent effects. *J Am Chem Soc* 127(7):2339–2350.
37. Sokolov AN, et al. (2011) From computational discovery to experimental characterization of a high hole mobility organic crystal. *Nat Commun* 2:437.
38. Ferretti A, Ruini A, Molinari E, Caldas MJ (2003) Electronic properties of polymer crystals: The effect of interchain interactions. *Phys Rev Lett* 90(8):086401.
39. Johansson E, Larsson S (2004) Electronic structure and mechanism for conductivity in thiophene oligomers and regioregular polymer. *Synth Met* 144(2):183–191.
40. Hoffmann ST, et al. (2013) How do disorder, reorganization, and localization influence the hole mobility in conjugated copolymers? *J Am Chem Soc* 135(5): 1772–1782.
41. Grozema F, Siebbeles L, Gelinck G, Warman J (2005) The opto-electronic properties of isolated phenylenevinylene molecular wires. *Molecular Wires and Electronics*, Vol 257, *Topics in Current Chemistry* (Springer, Berlin), pp 851–853.
42. Hendry E, et al. (2005) Interchain effects in the ultrafast photophysics of a semiconducting polymer: THz time-domain spectroscopy of thin-films and isolated chains in solution. *Phys Rev B* 71(12):125201.
43. Pearson DS, Pincus PA, Heffner GW, Dahman SJ (1993) Effect of molecular weight and orientation on the conductivity of conjugated polymers. *Macromolecules* 26(7): 1570–1575.
44. Hu T, Shklovskii BI (2006) Theory of hopping conductivity of a suspension of nanowires in an insulator. *Phys Rev B* 74(5):054205.
45. Hu T, Shklovskii BI (2006) Hopping conductivity of a suspension of flexible wires in an insulator. *Phys Rev B* 74(17):174201.
46. Kumar S, Murthy JY, Alam MA (2005) Percolating conduction in finite nanotube networks. *Phys Rev Lett* 95(6):066802.
47. Pimparkar N, Alam MA (2008) A bottom-up redefinition for mobility and the effect of poor tube-tube contact on the performance of CNT nanonet thin-film transistors. *IEEE Electron Device Lett* 29(9):1037–1039.
48. Hu T, Grosberg AYu, Shklovskii BI (2006) Conductivity of a suspension of nanowires in aweakly conducting medium. *Phys Rev B* 73(15):155434.
49. Koslover EF, Díaz de la Rosa MA, Spakowitz AJ (2011) Theoretical and computational modeling of target-site search kinetics in vitro and in vivo. *Biophys J* 101(4):856–865.
50. de la Rosa MA, Koslover EF, Mulligan PJ, Spakowitz AJ (2010) Dynamic strategies for target-site search by DNA-binding proteins. *Biophys J* 98(12):2943–2953.

Supporting Information

Noriega et al. 10.1073/pnas.1307158110

SI Text

Simulations

The methods used to implement the model and simulations are described in detail in this section. First, we create a random polymer chain conformation described by the worm-like chain model (1–6). The orientation of the initial chain segment is chosen at random. For each following segment, the orientation relative to the previous segment is defined by the bending and rotation angles, θ and ϕ. The bending angle $0 \le \theta \le \pi$ was chosen from a probability distribution taking into account the energetic penalty associated with that elastic deviation at room temperature as follows:

$$p(\theta) = \frac{\epsilon \sin\theta}{2 \sinh \epsilon} \exp[\epsilon \cos\theta]. \quad \text{[S1]}$$

After determining the bending angle, any value for the rotation about the chain axis was chosen, $0 \le \phi \le 2\pi$. This was repeated until the chain had the desired contour length L.

To simulate the long-time behavior of charges, we implemented the following algorithm for each value of electric field and temperature: (1) create a random chain conformation, (2) calculate the transfer rates between all of the sites on the chain using semiclassical Marcus theory (7, 8), (3) place a charge in a random site along the chain, (4) create the matrix that defines the set of algebraic equations in Laplace space, (5) solve the matrix equations and normalize the result vector by k_{hop}, (6) calculate the expected displacement of the charge in that chain as $\Delta z = \sum_i p_i z_i - z_{start}$, and (7) repeat steps 1–6 for a large number of chains and average the displacements. The mobility was obtained as the ensemble average of Δz multiplied by the hopping rate and divided by the electric field.

For the Monte Carlo simulations, we implemented a version of the Gillespie algorithm (9, 10): (1) create a random chain conformation, (2) calculate the transfer rates between all of the sites on the chain, (3) place a charge in a random site along the chain, (4) out of the three possible hopping outcomes—two neighbors on the same chain, and one on a different chain—randomly select the destination and hopping time. For neighbors (A, B, C) with transfer rates k_A, k_B, k_C, the probability of hopping to A is proportional to k_A/k_{tot}, where $k_{tot} = k_A + k_B + k_C$ is the total hopping rate. The hopping time is selected randomly from an exponential distribution with decay time $1/k_{tot}$. (5) Repeat step 4 until the destination site is on a different chain; (6) repeat steps 1–5 until the charge hops the desired number of times. This algorithm yields a trace for the position as a function of time for a single charge migrating through the material. To obtain an ensemble average, this process must be repeated for a large number of charges.

Convergence checks were performed to ensure that the simulations did not have artifacts relating to undersampling the chain conformations, as well as the number of charges tracked for the Monte Carlo simulations.

The function that is minimized in our simulated annealing procedure is the difference between the experimental and predicted mobilities, in a log scale, as follows:

$$R^2 = \frac{1}{N} \sum_{i=1}^{N} \left[\log\left(\frac{\mu_{experiment}}{\mu_{simulation}} \right) \right]^2. \quad \text{[S2]}$$

This allows for the description of mobility data over orders of magnitude, whereas if the linear mobility values were used in the fitting routine, larger mobilities would be weighed much more strongly than small mobility values. In a simulated annealing routine, a given perturbation to the fitting parameters is kept if it improves the overall fit to the data. If a perturbation decreases the quality of the fit, it is kept with a probability that decays exponentially with the change in the fitting residues normalized by a simulation temperature (here, $T_{sim} = 5 \times 10^{-4}$). The uncertainties in the parameter values were obtained by calculating the variance of the parameter space sampled with $T_{sim} = 1$.

Analytical Expression for the On-Chain Mobility

The mobility of a charge q moving along a segment of length l_0 oriented at an angle θ with the electric field $\vec{F}$ will be determined by the distance it travels along the field, $l_0 \cos\theta$, and the rate at which it is transferred, $k(\theta)$. Defining $\rho = \cos\theta$, and averaging over all possible orientations it is possible to write the following:

$$\begin{aligned}
\mu &= \frac{\langle v_z \rangle_\rho}{F} \\
&= \frac{2\pi}{\hbar} \frac{J_0^2 l_0}{F\sqrt{4\pi\lambda_0 k_B T}} \exp\left[-\frac{\lambda_0}{4k_B T} \right] \\
&\quad \times \int_0^1 \rho \exp\left[-\frac{F^2 q^2 l_0^2}{4\lambda_0 k_B T} \rho^2 + \frac{F q l_0}{2k_B T} \rho \right] \mathrm{d}\rho \\
&= \frac{\pi \lambda_0 J_0^2}{\hbar F^3 q^2 l_0} \left\{ \mathrm{erf}\left[\frac{1}{2} \sqrt{\frac{\lambda_0}{k_B T}} \left(\frac{F q l_0}{\lambda_0} - 1 \right) \right] + \mathrm{erf}\left[\frac{1}{2} \sqrt{\frac{\lambda_0}{k_B T}} \right] \right\} \\
&\quad + \frac{J_0^2 \sqrt{4\pi\lambda_0 k_B T}}{\hbar F^3 q^2 l_0} \exp\left(-\frac{\lambda_0}{4k_B T} \right) \left[1 - \exp\left(\frac{F q l_0}{2k_B T} \left(\frac{F q l_0}{2\lambda_0} - 1 \right) \right) \right].
\end{aligned} \quad \text{[S3]}$$

Eq. **S3** yields an analytical expression that involves only l_0, J_0, λ_0, F, T, and physical constants. The on-chain mobility increases for larger fields due to the increasing driving force for charge transfer, and artificially increases at very low fields due to the inverse field dependence of mobility—even though charges move more slowly, the v/F ratio increases as $F \to 0$. Thermal activation increases the rate of charge transfer, and thus the mobility as the temperature increases.

The distance over which this large on-chain mobility is sustained depends on the mechanical properties of the polymer chains. Strongly disordered conformations (low bending modulus) result in short correlation lengths of the segment orientation and short distances between kinks in the chain. Increasing the stiffness of the polymer backbone should result in a larger role of the on-chain mobility for charge transport.

Effect of Molecular Properties and Processing Conditions on Charge Transport

The usefulness of our model is directly related to the lessons we learn through its simplicity. It is possible to predict how changes in materials properties, both electronic and microstructural, result in observable differences in the charge transport behavior. To explore this point further, we ran simulations where we systematically varied the parameters of our model. In each panel of Fig. S1, only one parameter was modified (ε for A and D; J_0 for B and E; J_{hop} for C and F), whereas all other model parameters

were kept constant at the values reported for poly(spiro-bifluorene) in the main text.

One parameter that is easy to access experimentally is the bending modulus ε (or persistence length) of the polymer chains. Mechanical stretching of a polymer film is one way to align the polymer chains and induce a more rigid conformation. As shown in Fig. S1, this manipulation would have dramatic effects on the device-scale charge transport properties of the film, with little to no effect on the small-scale electronic processes. This strategy has been shown to increase the conductivity of conjugated polymer films by aligning individual polymer chains (11).

A usual approach for the molecular design of polymeric semiconductors is the improvement of the intrachain electronic coupling (J_0). With our model, it is possible to show that the most dramatic effects of this approach are at the local scale, not the device scale. The short-range ultrafast mobility is most affected by changes in J_0, with only modest changes in the device-scale mobility.

A natural parameter to tune to improve long range charge transport is the interchain electronic coupling (the interchain charge transfer integral, J_{hop}). This can be done by improving molecular packing and orbital overlap. As expected, improving interchain transport only affects the mobility at longer scales.

1. Yamakawa H (1997) *Helical Wormlike Chains in Polymer Solutions* (Springer, Berlin).
2. Van Der Maarel JRC (2008) *Introduction to Biopolymer Physics* (World Scientific, Singapore).
3. Spakowitz AJ, Wang Z-G (2004) Exact results for a semiflexible polymer chain in an aligning field. *Macromolecules* 37(15):5814–5823.
4. Spakowitz AJ, Wang Z-G (2005) End-to-end distance vector distribution with fixed end orientations for the wormlike chain model. *Phys Rev E Stat Nonlin Soft Matter Phys* 72(4 Pt 1):041802.
5. Spakowitz AJ (2006) Wormlike chain statistics with twist and fixed ends. *Europhys Lett* 73(5):684.
6. Mehraeen S, Sudhanshu B, Koslover EF, Spakowitz AJ (2008) End-to-end distribution for a wormlike chain in arbitrary dimensions. *Phys Rev E Stat Nonlin Soft Matter Phys* 77(6 Pt 1):061803.
7. Marcus RA, Sutin N (1975) Electron-transfer reactions with unusual activation parameters - treatment of reactions accompanied by large entropy decreases. *Inorg Chem* 14(1): 213–216.
8. Marcus RA, Sutin N (1985) Electron transfers in chemistry and biology. *Biochim Biophys Acta* 811(3):265–322.
9. Gillespie DT (1977) Exact stochastic simulation of coupled chemical reactions. *J Phys Chem* 81(25):2340–2361.
10. Gillespie DT (1976) A general method for numerically simulating the stochastic time evolution of coupled chemical reactions. *J Comput Phys* 22(4):403–434.
11. Pearson DS, Pincus PA, Heffner GW, Dahman SJ (1993) Effect of molecular weight and orientation on the conductivity of conjugated polymers. *Macromolecules* 26(7): 1570–1575.

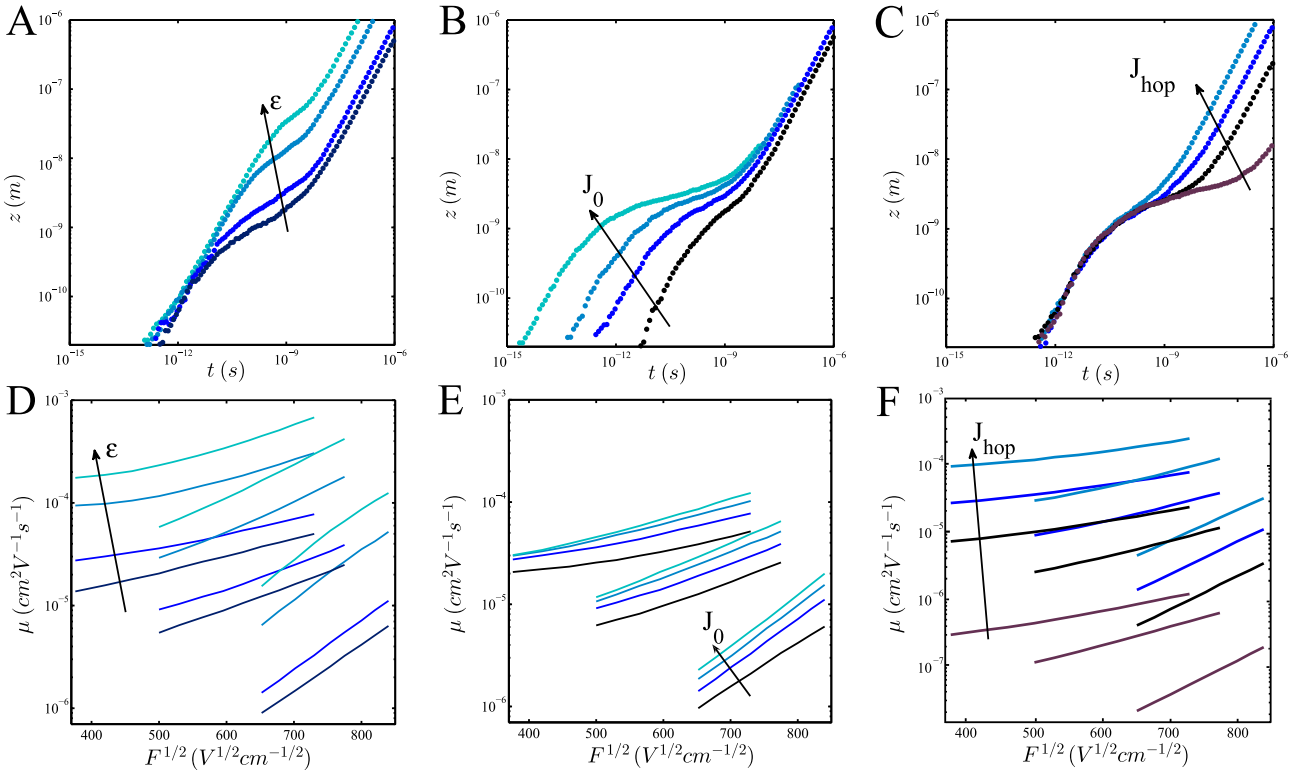

Fig. S1. Effect of a select group of parameters on the multiscale charge transport properties (*A–C*) and charge mobility as a function of temperature and electric field (*D–F*). The Monte Carlo simulations of charge transport used a voltage of 8 V at room temperature and a film thickness of 100 nm. The temperatures used for the transfer curves in the bottom row were 343 K, 263 K, and 173 K. (*A* and *D*) The arrows mark the direction of increasing chain stiffness $\epsilon = \{0.087, 1.73, 17.36, 173.6\}$. (*B* and *E*) The arrows mark the direction of increasing interchain charge transfer integral $J_0 = \{15, 45.6, 136, 456\}$ meV. (*A* and *D*) The arrows mark the direction of increasing intrachain charge transfer integral $J_{hop} = \{0.03, 0.17, 0.34, 0.69\}$ meV. In each pair of graphs, only one parameter is modified and all other model parameters are kept at the values found for poly(spiro-bifluorene) in the main text.